Enviado: 23/08/2020 *Recibido: 02/09/2020* *Aceptado: 15/10/2020*

UNIVERSIDAD DISTRITAL FRANCISCO JOSE DE CALDAS

VISIÓN ELECTRÓNICA

Algo más que un estado sólido

https://doi.org/10.14483/issn.2248-4728

VISIÓN ELECTRÓNICA

A CASE-STUDY VISION

Distributed Fault Diagnosis System based on Wireless Sensor Networks

Sistema de Diagnóstico Distribuido de Fallas basado en redes inalámbricas de sensores

Jairo Andrés Caballero-Peña[1], Javier Alveiro Rosero-García[2]

Abstract

This article presents the development of a distributed fault diagnosis and monitoring system whose remote nodes are responsible for data collection and distributed analysis to identify problems that could lead to critical faults in industrial processes or systems. The developed intelligent remote node was implemented with MCU LPCXpresso54114 connected to a ZigBee protocol wireless sensor network through XBee communication module. The gateway node is a Raspberrry PI with HTTP communication and JSON format to the PI System industrial monitoring system database. Motor Current Signature Analysis (MCSA) was implemented and validated to identify interturn faults of induction motors. The developed platform is a tool to perform comparison and validation of analysis techniques, indicators, and fault classification, because there are different combinations that can be applied to improve diagnosis reliability,

[1] BSc. in Electronic and Electrical Engineering, Universidad Nacional de Colombia, Colombia. MSc. in Electrical Engineering, Universidad Nacional de Colombia, Colombia. Current position: Young researcher, Electrical Machines & Drives - research group. Technical support engineer, Staekka SAS, Colombia. E-mail: jacaballerop@unal.edu.co ORCID: https://orcid.org/0000-0002-5350-4785

[2] BSc. in Electrical Engineering, Universidad del Valle, Colombia. PhD. in Electronic Engineering, Universidad Politécnica de Cataluña (UPC), Spain. MSc. in Administration, Universidad Nacional de Colombia, Colombia. Current position: Tenured professor and director of Electrical Machines & Drives - research group, Department of Electric and Electronics Engineering, Universidad Nacional de Colombia, Colombia. E-mail: jaroserog@unal.edu.co ORCID: https://orcid.org/0000-0003-2690-4772

Cite this article as: J. A. Caballero Peña, J. A. Rosero García, "Distributed Fault Diagnosis System based on Wireless Sensor Networks", *Visión Electrónica*, vol. 14, no. 2, July 2020. https://doi.org/10.14483/22484728.17058

fault observability, differentiation between fault conditions, classification accuracy, tolerance to transients, sensitivity, among others.

Keywords: Distributed Analysis, Fault Diagnosis, Induction Motor, Motor-Current Signature Analysis, Stator Current, Wireless Sensor Networks, ZigBee.

Resumen

En este artículo presenta el desarrollo de un sistema de monitoreo y diagnóstico distribuido cuyos nodos remotos se encarguen de la recolección de datos y su posterior análisis para la identificación de anomalías que representen fallas críticas para el proceso o sistema industrial. El dispositivo desarrollado como nodo remoto inteligente se implementó con MCU LPCXpresso54114 con conexión a una red inalámbrica de sensores basada en protocolo ZigBee mediante tarjetas de comunicación XBee. El nodo concentrador está compuesto de una tarjeta Raspberrry PI con comunicación mediante protocolo HTTP y formato JSON a la base de datos del sistema de monitoreo industrial PI System. Se implementó y validó el acondicionamiento de señal para la medición de corrientes de estator (MCSA) que permitió identificar fallas entre espiras de motores de inducción tipo jaula de ardilla. La plataforma presentada finalmente es una herramienta para realizar comparación y validación de técnicas de análisis, indicadores y de clasificación de fallas, puesto que existen diversas combinaciones que pueden ser aplicadas con el fin de mejorar la confiabilidad del diagnóstico, la observación de la falla, la diferenciación entre condiciones de falla, la precisión de la clasificación, la tolerancia a transitorios, sensibilidad, entre otros.

Palabras clave: Análisis distribuido, Diagnóstico de fallas, Motor de Inducción, Motor-Current Signature Analysis, Corriente de estator, Redes inalámbricas de sensores, ZigBee.

1. Introduction

Research on motor fault diagnosis has become relevant nowadays as it allows the identification of problems prior to a major event that affects the overall performance of an electric motor-driven system (EMDS), so as to reduce production downtimes, economic losses, and the impact on the useful life of the plant and equipment [1][2][3]. Eighty percent of the motors used industrially are induction motors and 21% of the faults that occur in electric motors is short-circuit faults in the stator [4]. For this reason, the study of these faults has made significant progress regarding their early diagnosis in order to identify interturn faults, which are caused by deterioration of the insulation and lead to more serious faults: ground faults [5].

Monitoring systems generally employ various sensors that report information to a server that performs centralized analysis based on historical data and its behavior. Currently, the use of wireless sensor networks (WSN) and their integration with system on chip (SoC) devices make a distributed diagnosis possible [6], in which the remote node is responsible for a total diagnosis of the fault and reports only the status of the equipment or carries out a partial analysis first and then a more advanced analysis. This reduces maintenance costs, facilitates the installation of new signals, provides flexibility in network and system configuration, reduces the power consumption of the remote node [6][7], and ensures greater communication security and reliability [3].

There is a great variety of methods for extracting parameters or fault indicators in which motor-current signature analysis (MCSA) is the most implemented on diagnostic systems, as it is a non-invasive process, supports different types of faults (breaks, stator, driver, or mechanical load) and involves a low cost of the integration of the sensors (without special requirements) [8]. Additionally, the behavior of this type of analysis is characterized by faults and diverse analysis techniques for identifying the presence of a fault [9]. MCSA has proved to be suitable

for implementation in programmable devices such as MCU and DSP [10][11][12], As for [13], a real-time analysis platform with centralized processing was developed; it was based on techniques such as Fast Fourier Transform (FFT), Discrete Wavelet Transform (DWT), Hilbert-Huang Transform (HHT), or the Discrete Harmonic Wavelet Transform (DHWT) [14], whose memory and processing capacity requirements are acceptable.

Analysis techniques show the characteristic behavior of a fault, but only data classification techniques help to determine the presence or probability of fault as well as its location or severity [15][16][17][18], thereby improving the accuracy and diagnostic precision. In programmable devices the proposed analysis techniques include behavior limits based on historical records (Threshold) [11][18], artificial neural networks (ANN) [17], support vector machines (SVM) [10][19] and probabilistic tools [20].

Diagnostic techniques evolve constantly as improvements are continually proposed to enhance sensitivity, accuracy, differentiation from other types of faults, or speed of analysis [5][21][22][23][24], these improvements include linear transformations as sequence components, dq0, quadrature or Park transformation, alternative data classification tools (artificial intelligence) or big data analysis. Therefore, the objective of this study was the development and implementation of a motor-current signature analysis (MCSA) based on a WSN through ZigBee protocol for remote diagnosis of faults in induction motors, in order to evaluate the performance of analysis techniques, fault classification, and proposed indicators. The proposed system performed diagnosis through SVM based on fault indicators extracted by FFT and DWT from the measured stator currents.

2. Architecture of the diagnostic system

The general operation of the system consists of remote nodes and gateways communicated wirelessly with ZigBee protocol through XBee communication modules, which simplify the

integration, configuration, and use of the private network by having dedicated libraries and application programming interfaces (APIs). Figure 1 shows the general structure: the gateways finally have access to the unified database, so data and alarms can be routed through any of the gateway nodes.

In each remote node, the variables associated with the motors are measured and then processed; the information on the faults is reported to the gateways afterwards. The associated processing can have three levels of abstraction: reporting of the sampled data of a specific period (original signal), reporting of signal indicators and characteristic parameters such as RMS value, DC value, harmonics, or indicators for centralized fault diagnosis. The third level of abstraction corresponds to the reporting only of the result of the diagnostic process, i.e. the output vectors of the process carried out in the classification of the fault based on the previously calculated indicators [6]. Each remote node has the structure described in Figure 2: there is a signal conditioning capable of receiving current or vibration signals and a microcontroller responsible for the analysis.

Figure 1. System architecture.

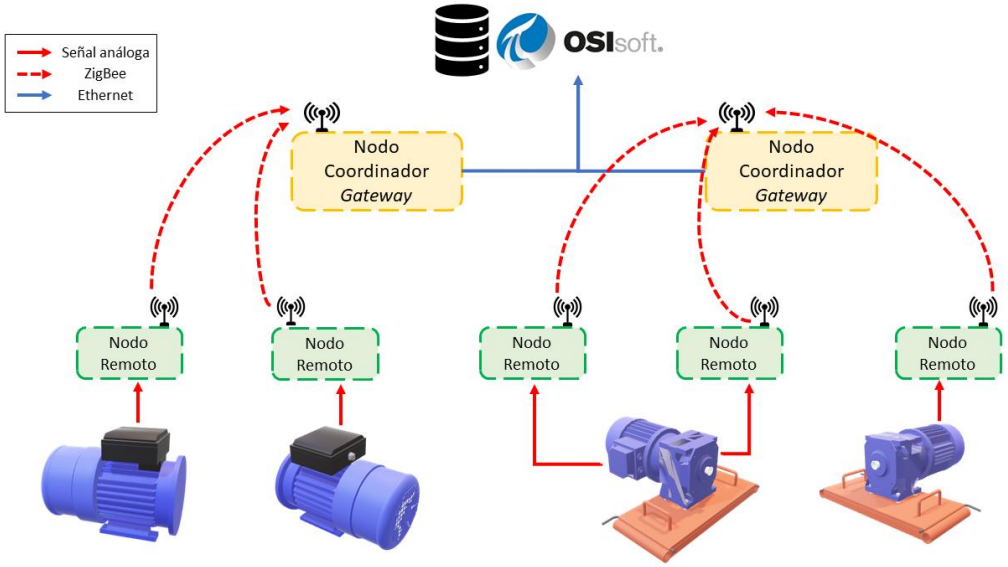

Source: own.

Figure 2. Remote node structure.

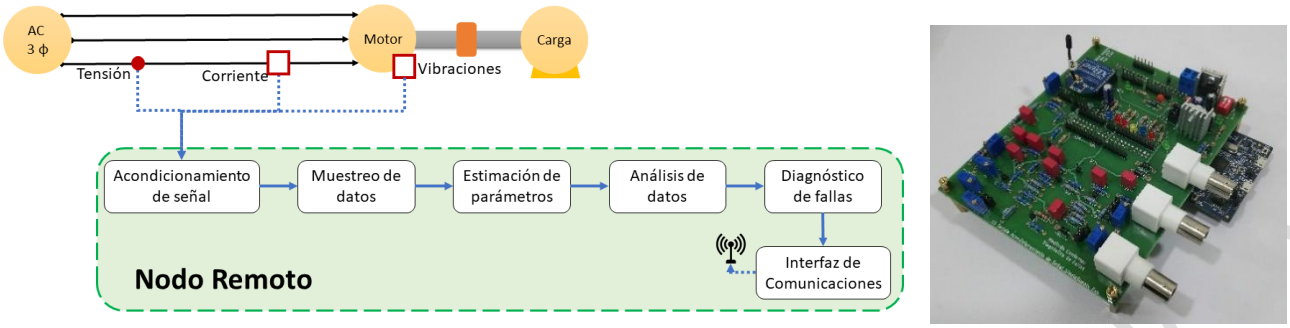

Source: own.

The communication interface of the remote node is an XBee node configured as a slave, which is accessed through the UART serial port by means of structured messages in API format; this allows the identification of sent messages, verification of the sent message, forwarding of unconfirmed frames, retransmission of data between nodes, message addressing, channel protection, data protection, message integrity, selection of the least noise channel, and node configuration.

The purpose of the gateway is to collect information and report it to the industrial monitoring system (PI system database), which has data management and visualization tools, access interfaces, and its own storage manager. Like the remote node, an XBee module configured as a gateway for UART serial communication in API mode is used. Its configuration includes the automatic search for a channel that is not occupied and has a low noise level.

With the proposed architecture, it is possible to monitor several variables of the same EMDS with different remote nodes and to make a diagnosis in the gateway based on multiple signals in a centralized manner. By having more information from the same motor, this data fusion process manages to improve the reliability of the diagnosis [3][6][25].

The subsequent data storage process is simultaneously performed locally (log files) for debugging and on the server through the HTTPS-based PI Web API. Once the data is stored

in the database, several queries are made to create the monitoring user interfaces, the periodic data reporting, and the alarm reporting to the system or maintenance operators. The tools used to provide access to information are PI Coresight for web visualization without software requirements, PI ProcessBook for execution on equipment with OSISoft licensed software, and again PI Web API as the interoperable solution for managing data to and from the database.

2.1. Implementation requirements

The requirements for the diagnosis system were validated and reviewed according to the previous implementation advances on MCU or similar equipment. For the different analyses it is necessary to have floating point units (e.g. TM4C1233H6PM [26]) to ensure the precision of the diagnosis or classification of the fault, in which standardized values are generally operated. In the case of implementing Wavelet through impulse response convolution, it is necessary to use enhanced processors such as parallel multiplication units, multiply-accumulate operation (MAC) features, or accumulators, available mainly in DSP.

For vibration-based bearing analysis, the typical analysis frequency is 256 Hz and MCSA is 5 kHz using 10-16 bit ADC [27]. Therefore, the sampling frequency was established as four times the maximum analysis frequency: $f_s = 20\ kHz$. The sampling process required an antialiasing filter that prevent the imaging, eliminate the subsampling of high frequency signals (multiples of the sampling frequency) and allows the passage of the target signal. At 25 kHz the attenuation should be maximum 74 dB, and at the cutoff frequency the attenuation should be 3 dB. There is no restriction on the type of filter used, but the offset introduced should be considered when including analyses involving the offset of the measured signals, for example impedance analysis. The given requirements are not achieved with a filter of order 10 or higher, equivalent to having at least 5 stages with amplifiers. Then, the cut-off band attenuation should be reduced to 33 dB or 35 dB, thereby lowering the complexity of the filter implementation. An

alternative to allow different sampling frequencies and to reach a filter up to order 8 on the same hardware in order to adjust the analysis according to the needs of the analysis is the use of switched-capacitor filters, which adjust their cut-off frequency according to the frequency of their control signal (clk). In this way, an additional requirement besides the MCU is the option to generate a clock signal adjustable in real time to control the Fc through software according to the needs of the sampling or the analysis. Therefore, an appropriate adjustment can be made to the sampling rate, the number of samples, and the use of the device memory with the aim of considering changes in various analysis techniques. For example, when analyzing interturn faults the frequencies associated with faults are cyclic in the spectrum at multiples of the synchronism frequency usually greater than 700 Hz, whereas for mechanical faults the frequencies to be reviewed are usually frequencies lower than those of the network (60 Hz).

2.2. Platform definition

A search and comparison of development platforms with low consumption MCU or DSP were performed and the following evaluation criteria were established: power consumption, configuration in sleep mode, current consumption in Stand By mode, serial communication modules, RAM and Flash memory, processor, floating point processing unit, number of cores, supply voltage, ADC channels, number of ADC bits, maximum sample rate, available inputs and outputs, communication ports, additional modules, available development cards, price, and libraries for development. The most important criteria were energy consumption due to the requirement to operate autonomously with batteries, the processor with a floating-point unit (fundamental condition), the estimated sampling frequency for six different signals, and the memory capacity. As for the latter, it was sought as much as possible in order to ensure the highest sample capacity (low-frequency analysis) and to store the temporal signals required in processes such as HHT (decomposition in empirical methods). As a result, the

LPCXpresso5411x series was selected, an LPC54114J256 MCU based on an ARM Cortex M4 processor with an ARM Cortex M0+ coprocessor. The corresponding NXP development board is an OM13089 (LPCXpresso54114), which can be programmed on C++ via USB serial communication with its bootloader.

3. Implementation of the diagnostic system

3.1. Signal conditioning

The signal conditioning (see Figure 3) was developed for coupling signals delivered by a current clamp (voltage transducer) or an accelerometer with voltage output 0 V to 5 V. A high impedance rail-to-rail operational amplifier (low offset and noise) was used for each phase to avoid unwanted signal loading or attenuation problems. The first stage of offset was implemented with a non-inverting adder configuration in order to allow application with a single + 5V source (all stages with positive Vout). The final offset stage corresponds to the DC level correction introduced by the implemented switchable filter and should be calibrated before operation.

Figure 3. Block diagram of signal conditioning.

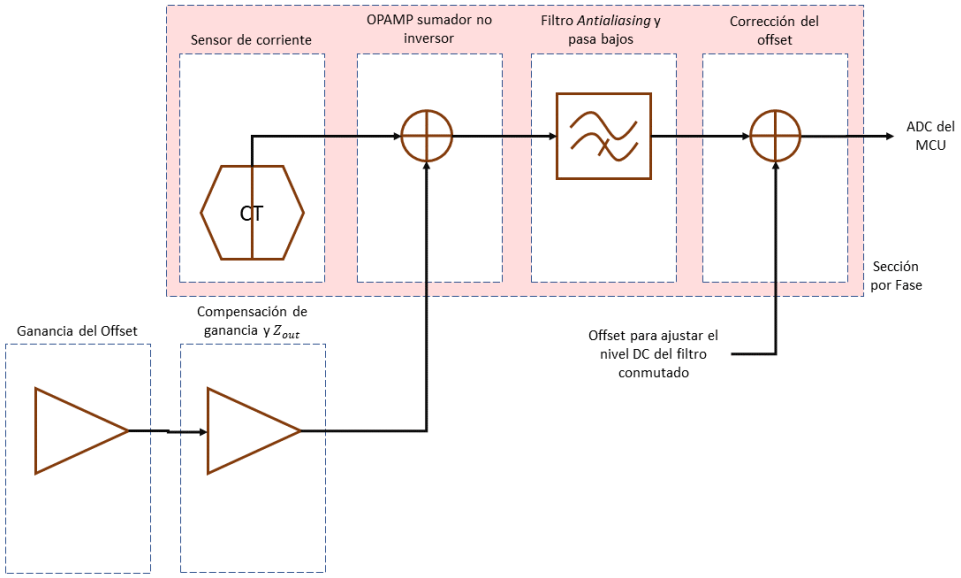

Source: own.

The MAX291 was used to adjust the cutoff frequency up to 25 kHz (or MAX295 for cutoff frequencies up to 50 kHz), male BNC connectors for male BNC connectors for connecting current clamps, low-power low-noise (high performance) OPA4188AID operational amplifiers, protection against overvoltage and transient reverse voltage that may reach the MCU's ADC inputs (clipper), Zener diodes to ensure a more stable offset in relation to the external variations of the power supply, and a power supply based on a single external voltage (9 V batteries) that generates a floating ground and achieves a symmetrical output (±5 V).

Laboratory tests were performed on the dynamic filter by introducing a TTL clock signal (clk) and sinusoidal variable input signals. Because the control signal is 100 times or 50 times f_c depending on the implemented switched-capacitor filter, the clk signal can be up to 2.5 MHz. A clk signal attenuation occurred due to the capacitive effect of the probe and parasitic capacitances on the PCB, which was corrected by changing the PCB substrate, performing a symmetric routing of the signal, and removing the VIA-hole in the prototype.

To verify the operation of the filter, the frequency sweep was performed for two different cutoff frequencies (f_c) with their respective control frequency (f_{clk}). Figure 4 shows the normalized frequency response in relation to f_c, with similar attenuation slopes and corner frequencies. The installed amplifier is the MAX 291 with a cutoff frequency range from 0.1 Hz to 25 kHz and a control ratio of 100:1; the observations showed that the frequencies that were not affected by the filter had a permanent attenuation due to the gain of the operational amplifiers to ensure the measurement range of the MCU. The attenuation at $f_{in} = 0\ Hz$ (DC values) is due to the filter introducing an offset associated with the filter operation. The typical attenuation expected in a low-pass filter at the cutoff frequency is -3 dB (gain 0.5 V/V), but the attenuation at the cutoff frequency of the switched-capacitor filter was found to be -1.196 and -1.366, $f_c = 10\ kHz$

and $f_c = 20\ kHz$, respectively. A correction was then made to the control frequency by 10% to ensure attenuation by shifting f_{clk} to a lower frequency.

Figure 4. Normalized transfer function of the dynamic filter for various f_c.

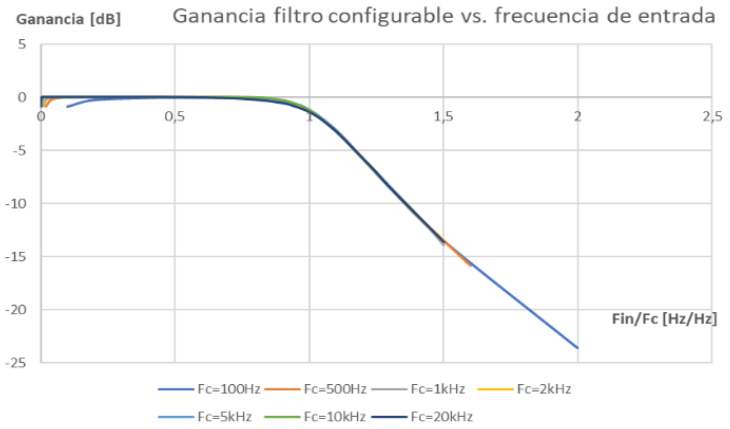

Source: own.

Table 1 shows the target cutoff frequency, the control frequency, the gain measured at the target cutoff frequency, and the gain at the corrected cutoff frequency. As can be seen, the attenuation of 3 dB is achieved by correcting f_c and, therefore, at least the control frequency should be adjusted by 10% for correct control.

Table 1. Comparison of the gain for different cutoff frequencies.

		Gain [dB]	
f_c [kHz]	f_{clk} [kHz]	$\frac{f_{in}}{f_c} = 1$	$\frac{f_{in}}{f_c} = 1.1$
0.1	10	-1.213	-3.161
0.5	50	-1.196	-3.188
1.0	100	-1.213	-3.201
2.0	200	-1.204	-3.188
5.0	500	-1.146	-3.071
10.0	1000	-1.196	-3.188
20.0	2000	-1.366	-3.201

Source: own.

Table 2 shows the calculated attenuation for each cutoff frequency adjusted. The average attenuation in the transition band is 80,332 dB/decade. These variations occurred because the

final section of the characteristic curve cannot be approximated to perfect straight lines (see Figure 4). This behavior can be confirmed in the datasheet [28] and can be approximated with three different slope lines.

Table 2. Comparison of the gain for different cutoff frequencies.

f_c	f_{clk}	Attenuation [$dB/decade$]
0.1	10	80.368
0.5	50	80.423
1.0	100	83.636
2.0	200	79.465
5.0	500	79.176
10.0	1000	78.463
20.0	2000	80.791

Source: own.

The phase angle characterization was performed by configuring two cutoff frequencies (Fc), 5 kHz and 20 kHz, taking into account that in the last stage of signal conditioning an amplifier performs a subtraction to adjust the offset, which introduces an inversion of the reflected signal into an additional 180-degree offset. In general, the response of the phase angle behavior of the Butterworth filter can be a linear approximation as the frequency of the input signal increases; however, it should not be considered as such in case detailed phase angle analysis is needed, since in the case of the switched-capacitor filter the error varies as the f_c or f_{clk} is modified and the non-linearities affect the zero crossing of the phase angle. The zero crossing should match $\frac{f_c}{2}$, but for $f_c = 5\ kHz$ it is $0.5857 * f_c$, i.e. 17.15% higher, and for $f_c = 20\ kHz$ the error is 14.73% above $\frac{f_c}{2}$.

Finally, to improve energy consumption efficiency the power supply of the systems should be high efficiency and independently controllable, so that the signal conditioning, the MCU, and the communication module can be operated in Wake-Up cycles. In this way, the elements of

the system operate only when required, i.e. data collection and data analysis or transmission, so as to maximize the time of use of the batteries [3].

3.2. Remote node

The software for the remote node employs several hardware modules with the ability to launch hardware interruptions to leave only the tasks of data analysis, data reporting, and communication network configuration in the main processor. Figure 5 and Figure 6 show the flow chart of the remote node and the interruption cycles in which the tasks of data sampling, storage of the measured channels, and control of energy consumption of the signal conditioning are performed (Wake Up, Sleep Mode).

Figure 5. Flowchart of the remote node software.

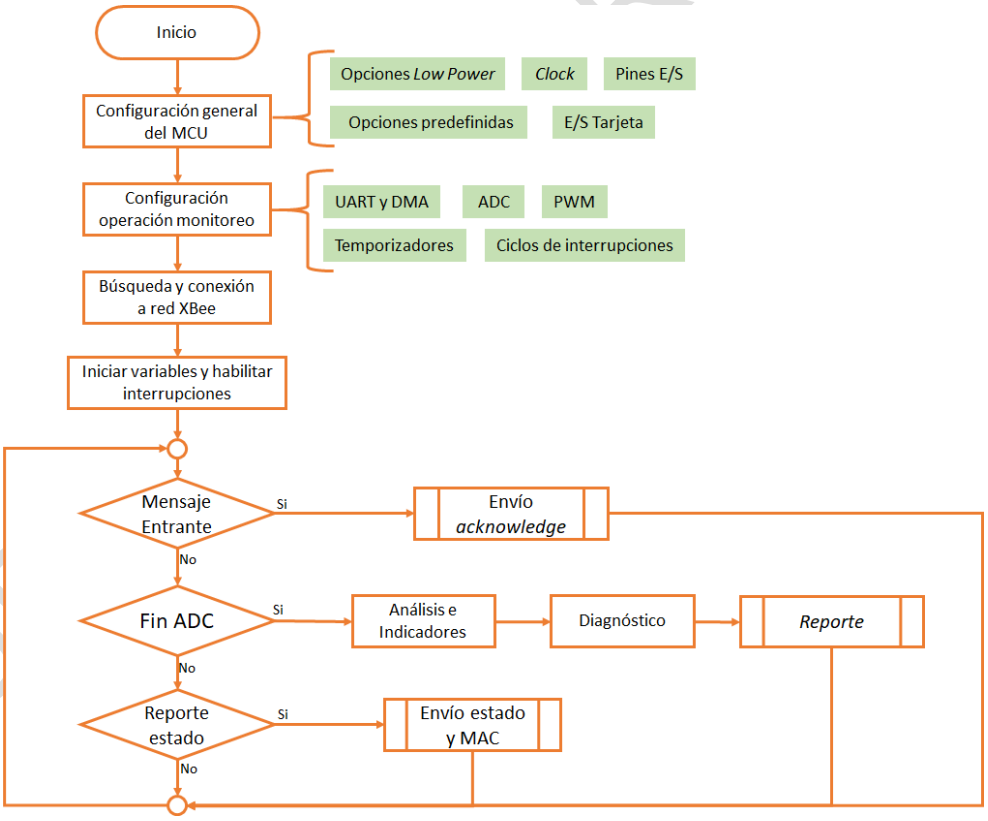

Source: own.

The development of the remote node software required the development and integration of libraries for the operation of the XBee communication module in API format via serial port. The

developed code involved employing the existing MCU[3] drivers related to the data sending through serial port by using the Direct Memory Access (DMA) block and the UART port. The advantages of using messages in API format include the use of broadcast messages, automatic network selection, message receipt acknowledgment (ack), dynamic data routing, and XBee network configuration.

Figure 6. Flowchart of the remote node software (hardware interruption cycle).

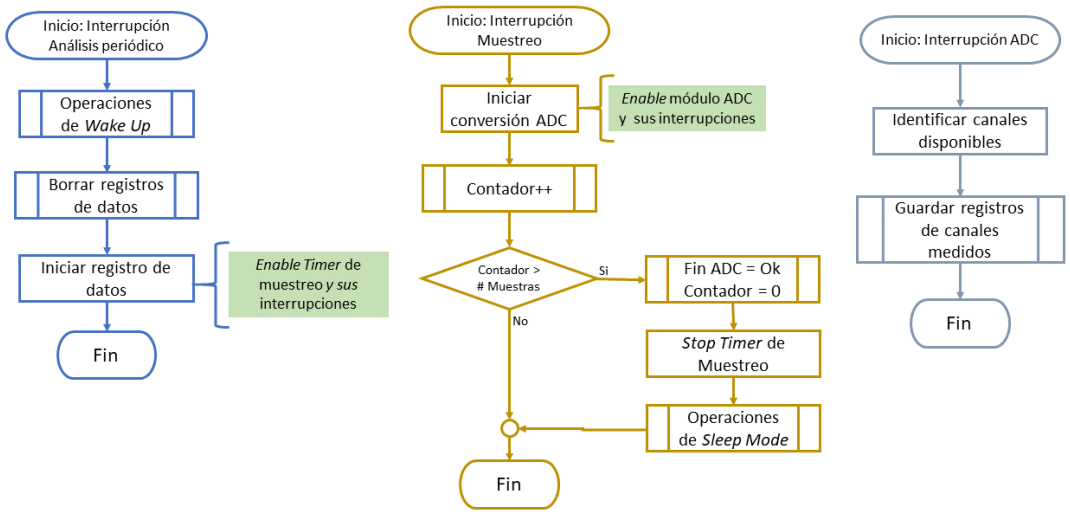

Source: own.

Based on the available drivers, the ADC block was adjusted for the sampling of up to 9 channels together with their respective timers to make data acquisition at the beginning of the periodic fault analysis and periodic status monitoring of the communication system. The switched-capacitor filter control signal was generated by the PWM block.

The section of the software corresponding to the analysis and the diagnosis required the configuration of the Cortex Microcontroller Software Interface Standard (CMSIS) libraries for the Cortex-M processor, with the aim of using the integrated functions for float type vector's operation. Based on these, the functions presented in the Table 3 were implemented.

[3] MCUXpresso IDE

Table 3. Analyses developed and integrated.

Basics, FFT and SVM	DWT
Measurement: ▪ RMS, AC, and DC value per phase Fast Fourier transform (FFT): complex numbers [A, Bi]: ▪ For 512, 1,024, 2,048, or 4,096 samples ▪ Results in complex numbers ▪ Absolute value and angle ▪ Main frequency extraction ▪ Peak value for frequency ranges ▪ Harmonics calculation Classification with SVM: ▪ Data reporting for training ▪ Kernel-based input vector estimation ○ Linear ○ Polynomial ○ Exponential ○ *rbf (radial basis function)* ○ *sigmoid* ▪ *Training validation*	Discrete Wavelet Transform (DWT) ▪ Decomposition level: Wavelet adjustable up to the number of samples ▪ Indicators per detail and calculated approximation: ○ Energy ○ Average ○ Variance ○ Standard deviation ○ Peak to peak value ○ Skewness ○ Kurtosis ▪ Boundary defect correction: ○ Complete with zeros ○ Constant ○ Symmetrical ○ Mirroring ○ Periodical ○ Antisymmetric ○ Anti-mirroring ○ *Smooth*

Source: own.

The proposed diagnosis was based on the extraction and calculation of fault indicators to later use them in an SVM for data classification. Offline training and validation of the SVM were performed with analysis libraries available in Python [29][30]. To classify new data collected in a distributed way by the remote node, it was necessary to develop a C++ compatible application, which applies only the decision equation through the Kernel used for training and the respective support vectors.

A frequency range self-adjusted to the main power frequency and based on the motor parameters was monitored; the frequency with the highest amplitude (frequency and absolute

value) was extracted as an indicator from this range. Based on previous fault frequency characterizations [31][32], the bandwidth to be monitored was restricted to load variations (s-slip changes) independent of the supply frequency. For FFT, the proposed indicators corresponded to each of the harmonics of the fundamental frequency: 60 Hz. As for DWT, the energy values were calculated for each approximation and detail that underpinned the fault diagnosis (training and prediction).

3.3. Gateway

The gateway should have a serial communication port, ethernet communication, configurable I/O ports, and capacity for the installation and execution of libraries in Python. Therefore, prototype development boards or industrial computers can be used. This study was carried out on a Raspberry Pi 3 Model B+ with a Debian operating system because of its easy prototyping. For the coordinator node or gateway, a shield was developed to integrate the XBee communication card (power supply, control and communication signals) into the I/O ports required to indicate alarms or generate alerts on the visual status of communications towards the remote nodes and/or towards the server (database and remote visualization).

An application was developed on Python[4] to configure the serial port of the Raspberry by verifying if it is available previously, otherwise the application does not run. The elements and objects necessary to use XBee were subsequently configured through its library for Python. In this process, a parallel execution process (callback) was configured to continuously monitor the input buffer of the serial port and to generate an interruption when receiving a message in API format, thereby reducing response times.

Figure 7 shows the block diagram of the process carried out on the main threat, and Figure 8 shows the process carried out in the background when receiving a message. The main

[4] https://python-xbee.readthedocs.io/en/latest/ and https://github.com/digidotcom/python-xbee

execution loop periodically monitors the status and availability of the XBee network (at least one remote device connected) and indicates the running status of the secondary message reception process through a blinker. In case of an error in any of the steps described above (exception), the software closes the serial port before end to avoid errors during the next launch or execution of the application. The process of restarting in case of an internal error was implemented in a script executed as a Watchdog (Crontab on Debian) every minute.

Figure 7. Flowchart of the gateway software.

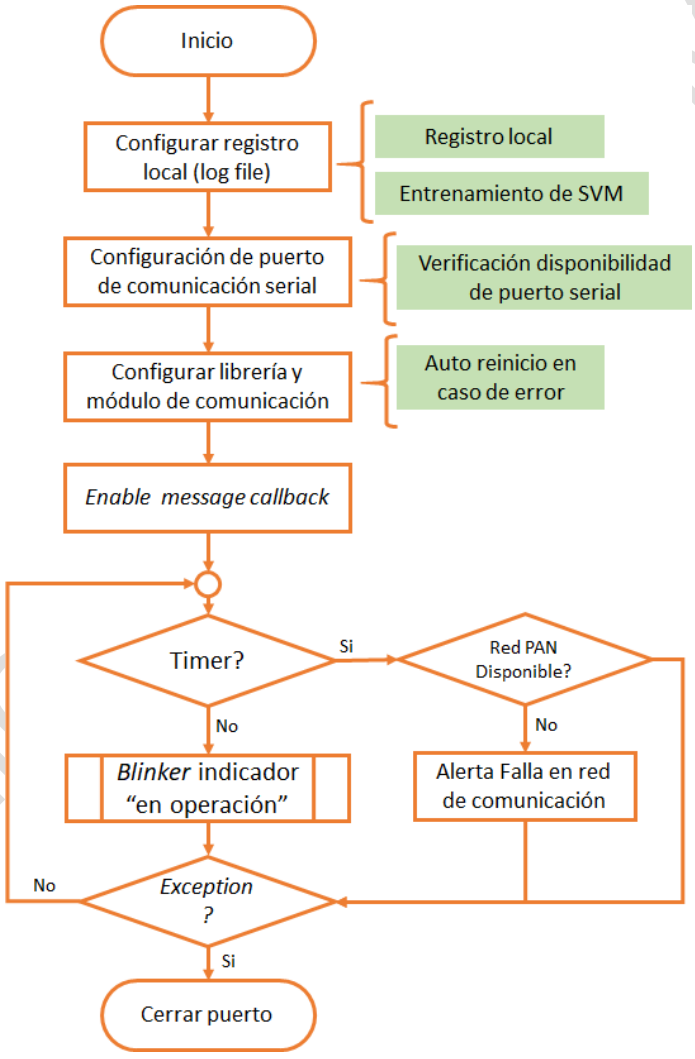

Source: own.

Figure 8. Flowchart of the gateway software: automatic interruption of received message.

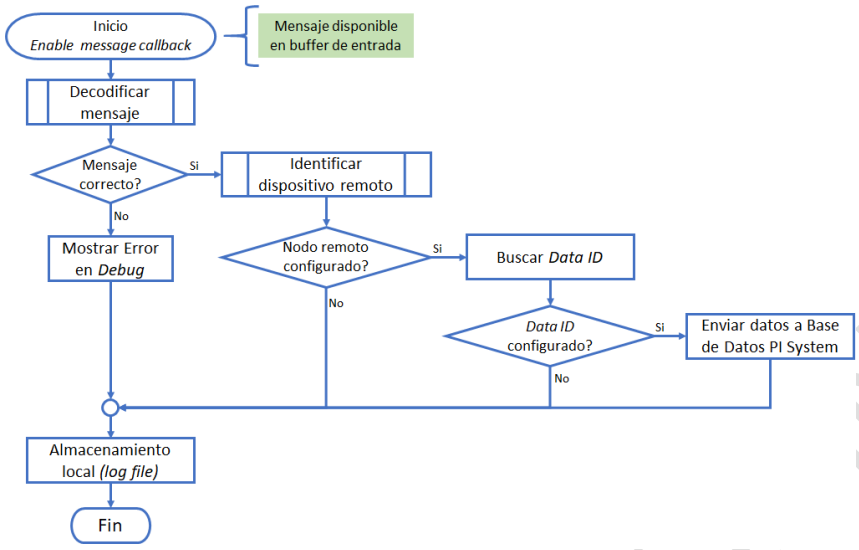

Source: own.

In the payload of each message, a format was established: two (2) characters of indicator identification or result (Data ID) and another four (4) characters for the corresponding value in float format; then the first validation checked that the data of the current message had a length of six (6) characters. Finally, the source address and the Data ID were used to find out if the received information were configured to be sent to the remote server for storage and visualization.

A JSON format was used to send information to the database via HTTP protocol (PI Web API interface): a different header pointing to a separate memory register should be sent per piece of data sent. By means of the Data ID, the respective header was searched in a Python dictionary of predefined headers to complete the HTTP address for the publication of the data. One of the restrictions to the reception of data, as well as the format of always sending a four-character float value, is to send a zero value. When sending a number in floating point format in hexadecimal format, registers are split to reduce the number of characters that are sent through the serial port. The resulting characters may be therefore null (0x00); this results in communication failures and erroneous decoding as nothing is found due to apparently shorter

data length. Then, the variation ranges of each piece of data reported were verified so that all of them were lower than one ($x < 1$) with some scale factor (forced filling of a float register) or never had zero values.

3.4. Server

Figure 9. Visualization of the diagnostic system in PI ProcessBook.

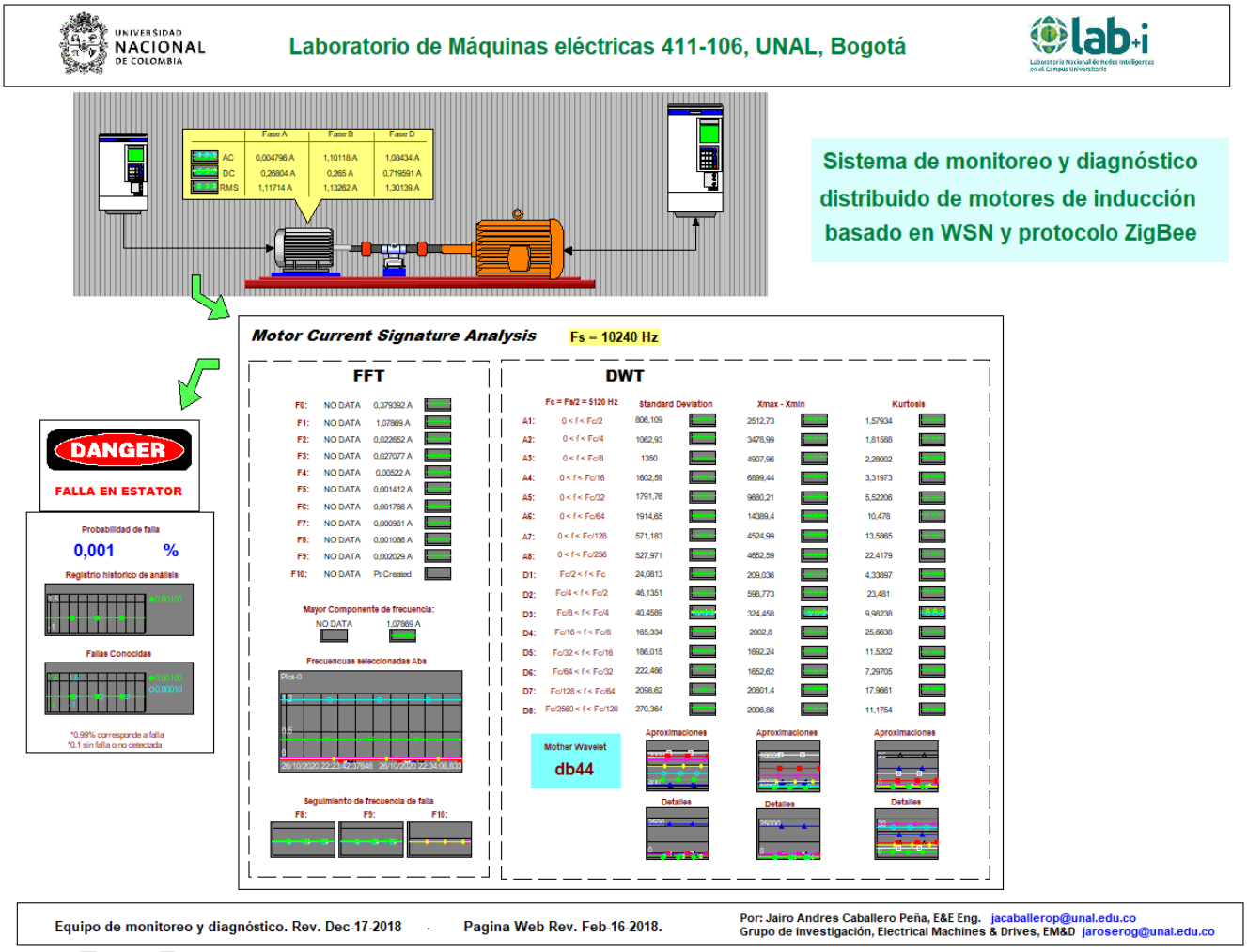

Source: own.

The operation of PI System requires a memory identifier or PI Point to be defined for each variable that will be stored so as to generate the data structure for correlating sites, machines, and sensors. Each Data ID was assigned a PI Point according to the storage needs and a description according to the analysis identifier to be reported in the data tree. The use of PI

Point allows different PI System applications to directly access the memory data for a faster operation; this helps to synchronize and separate data recording and loading tasks, data management (correlation of monitoring variables), fixed operations and analysis, and visualization interfaces.

One of the applications that operate directly with memory records is PI ProcessBook, which shows industrial process status variables in real-time and sends commands from the desktop, similar to the operation of a SCADA system. The visualization of the diagnostic system was developed on this interface: it shows the defined indicators, the status variables, and alerts in case of faults in the motor being monitored (see Figure 9); it is also possible to check the historical record of each variable to compare its behavior.

To use ProcessBook, it is necessary to install Pi System and its libraries in the monitoring computer, in addition to having a stable connection directly to the data server (Archive). As an alternative, for basic visualizations open to the public as other applications do, PI Vision (formerly PI Coresight) was used, whose operation is based on offering a web service for visualization in HTTP on a public IP. The latter was configured to provide the same visualization in ProcessBook within the interface of the Laboratory of Smart Grids lab+i at Universidad Nacional de Colombia.

4. System's test and verification

T The diagnostic system was implemented on a Siemens three-phase induction motor of 7.5 HP (5.6 kW) at 220 V, YY connection, nominal speed of 1,732 rpm, and FP of 0.73; this motor was adapted to generate interturn faults among 2, 4, and 6 turns of the stator in a controlled way (see Figure 10). Additionally, internal thermocouples were installed to monitor the winding temperature. This motor was located on a test bench to control torque and speed with the aim of adjusting the desired operation point of the motor for different tests.

Figure 10. Motor configuration with breakers for controlled interturn faults [32].

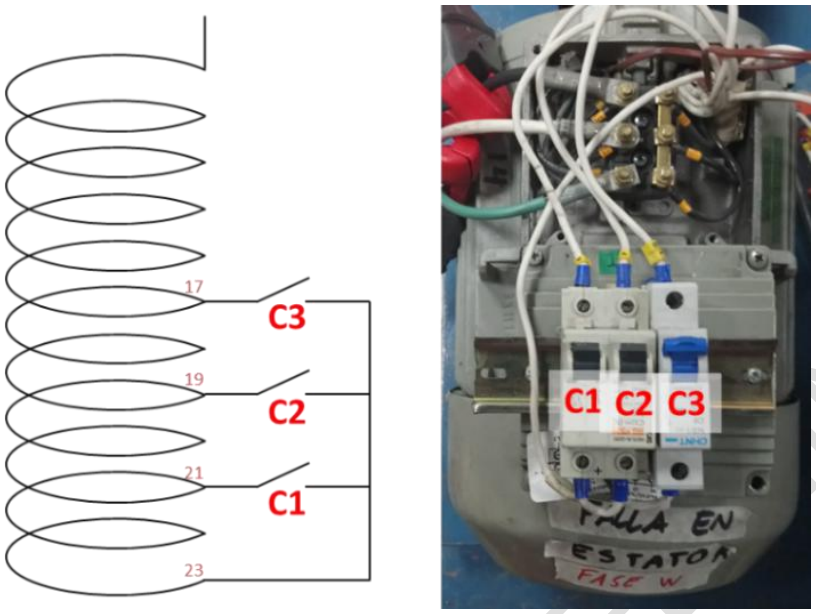

Figure 11 shows the test procedure for collecting training data and subsequently verifying operation. When setting the test condition, the torque and speed are adjusted to the reference conditions or those to be analyzed; in this case the speed was set at 100% to fully know the fault frequencies and the torque at 60% to prevent permanent damage of the motor insulation. For each piece of data recorded, an additional control signal was configured to indicate when a C1, C2 or C3 fault was applied; in this way, the data on fault and no faults was marked for analysis.

Figure 11. Test procedure for diagnosis.

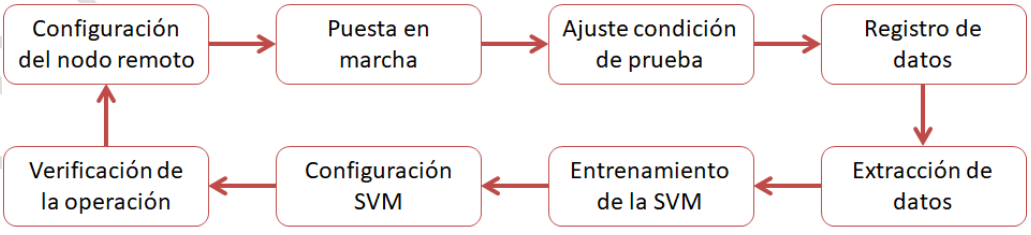

Source: own.

To verify the operation, the data was recorded again; in case of faults, the result of the SVM diagnosis was compared with the described control signal. Figure 12 shows an example: the

dotted signal indicates the result of the fault diagnosis (0 or 1) and the continuous line corresponds to the control signal to mark the fault; in this case a correct diagnosis of three C1 faults (2 turns) was achieved.

Figure 12. Expected result of fault diagnosis through PI Vision visualization.

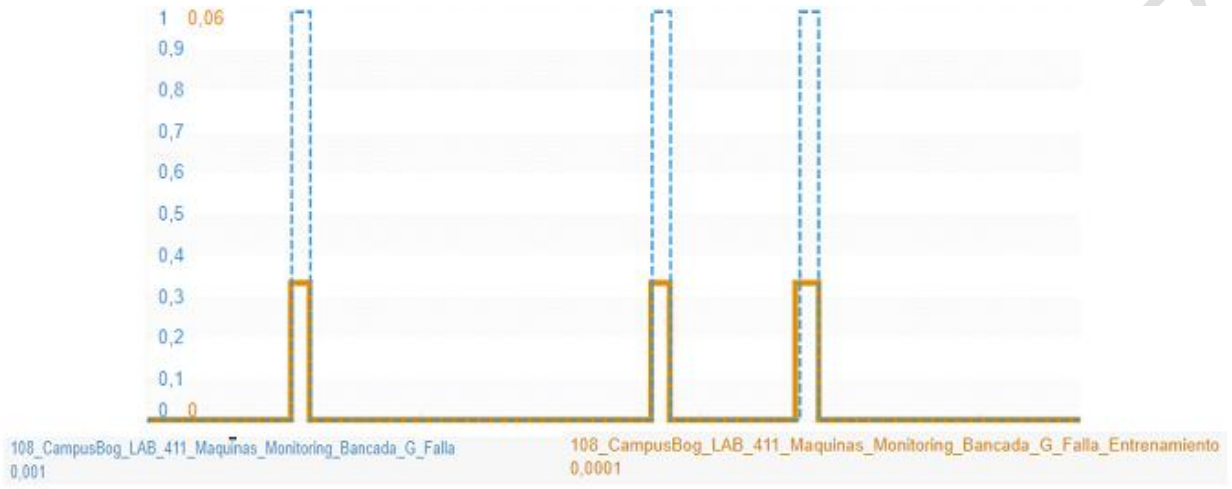

Source: own.

The diagnosis applied to validate the diagnostic system was based on the analysis of the current imbalance resulting from the application of an interturn fault. In Figure 13, the phase with the fault has an increase of 10%; therefore, the indicators used correspond to the AC value of the phase with fault compared to one of the other two, as shown in Figure 14.

Based on these indicators with their known data on fault and no fault, the SVM was configured to propose a linear classification kernel that achieved a score of 0.98 (see Figure 15). The validation tests showed that the fault was always detected during the conditions given in the laboratory (see Figure 12); however, it is worth mentioning that a current imbalance in the stator can be generated by more than one fault (AC/AC driver's faults, load imbalances, voltage imbalances, among others). Consequently, this method is appropriate to validate the system but not to make a correct diagnosis of the induction motor.

Figure 13. AC value of phase A and RMS of the main component in frequency through FFT of phase A for C1 fault with 100% speed.

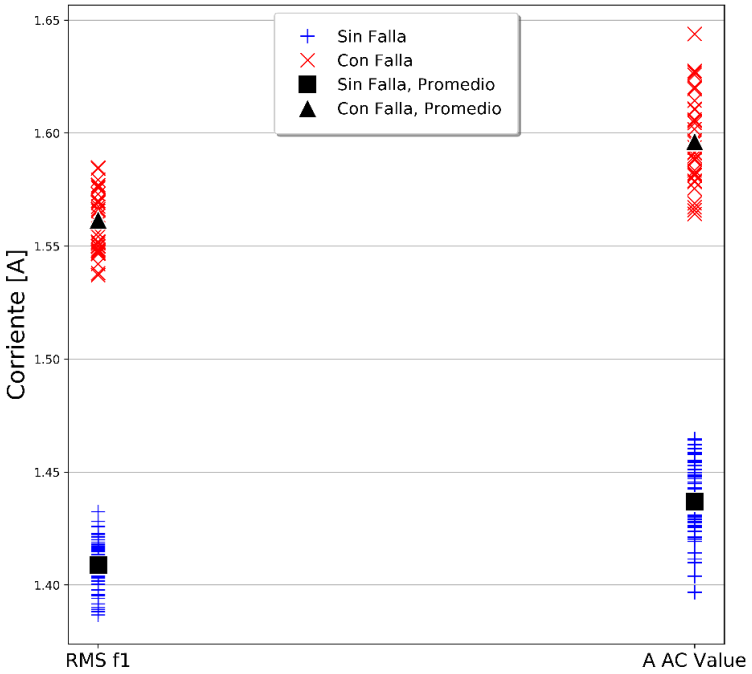

Source: own.

Figure 14. XY comparison of AC values of phase A and B for C1 fault with rated speed and 60% of the load.

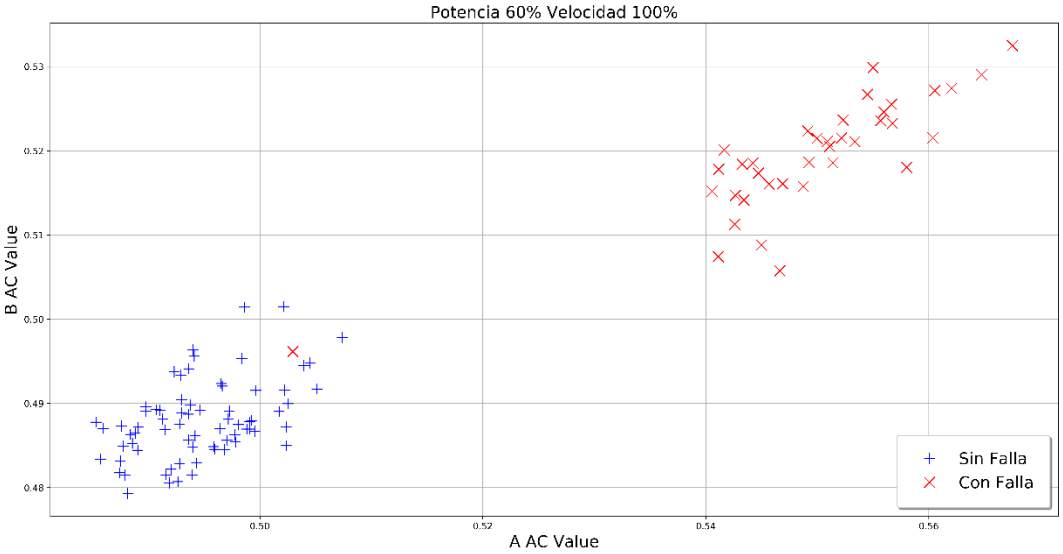

Source: own.

Figure 15. Normalized classification based on AC value of phase A and B for C1 fault with rated speed and 60% of load.

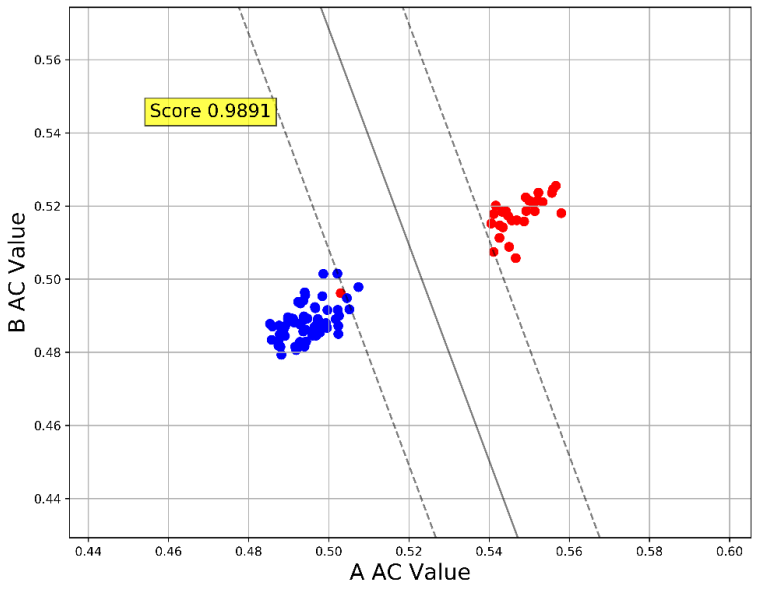

Source: own.

5. Conclusions

The platform was developed to identify interturn faults of the stator of an induction motor by calculating various indicators in a distributed manner to subsequently notify the result of the analysis to the industrial monitoring platform. The proposed structure aimed to reduce energy consumption and the bandwidth required for communication with the hub, changes in the needs of the server as less memory capacity is required, and the scalability of the system to integrate various monitoring devices.

The implementation of a wireless sensor network (WSN) integrated to the industrial monitoring system improves the reliability, access, and availability of data because of several gateways for data collection and routing through remote nodes. In addition, it improves tolerance to faults in the communication network, has greater capacity for distributed analysis, provides higher quality of information for decision making, and analyzes variables not previously considered in industrial systems.

Acknowledgments

Gratefulness to Electrical Machines & Drives – research group and UN Innnova program by academic division of Universidad Nacional de Colombia.

References

[1] J. P. Amaro, F. J. T. E. Ferreira, R. Cortesão, N. Vinagre, R. P. Bras, "Low cost wireless sensor network for in-field operation monitoring of induction motors", Proc. IEEE Int. Conf. Ind. Technol., pp. 1044-1049, 2010. https://doi.org/10.1109/ICIT.2010.5472560

[2] M. Bordasch, C. Brand, P. Gohner, "Fault-based identification and inspection of fault developments to enhance availability in industrial automation systems", IEEE 20th Conference on Emerging Technologies & Factory Automation (ETFA), 2015, pp. 1-8. https://doi.org/10.1109/ETFA.2015.7301515

[3] L. Hou, N. W. Bergmann, "Novel industrial wireless sensor networks for machine condition monitoring and fault diagnosis", *IEEE Trans. Instrum. Meas.*, vol. 61, no. 10, pp. 2787-2798, 2012. https://doi.org/10.1109/TIM.2012.2200817

[4] F. J. Ferreira, G. Baoming, A. T. de Almeida, "Reliability and operation of high-efficiency induction motors", IEEE/IAS 51st Ind. Commer. Power Syst. Tech. Conf., pp. 1-13, 2015. https://doi.org/10.1109/ICPS.2015.7266412

[5] A. Gandhi, T. Corrigan, L. Parsa, "Recent Advances in Modeling and Online Detection of Stator Interturn Faults in Electrical Motors", *IEEE Transactions on Industrial Electronics*, vol. 58, no. 5. pp. 1564-1575, 2011. https://doi.org/10.1109/TIE.2010.2089937

[6] N. W. Bergmann, L. Q. Hou, "Energy Efficient Machine Condition Monitoring Using Wireless Sensor Networks", Int. Conf. Wirel. Commun. Sens. Netw., pp. 285-290, 2014. https://doi.org/10.1109/WCSN.2014.65

[7] L. Hou, N. W. Bergmann, "Induction motor condition monitoring using industrial wireless sensor networks", Sixth Int. Conf. Intell. Sensors, Sens. Networks Inf. Process., pp. 49-54, 2010. https://doi.org/10.1109/ISSNIP.2010.5706739

[8] S. Nandi, H. A. Toliyat, X. Li, "Condition monitoring and fault diagnosis of electrical motors - A review", *IEEE Trans. Energy Convers.*, vol. 20, no. 4, pp. 719-729, 2005. https://doi.org/10.1109/TEC.2005.847955

[9] R. Windings, "In-service monitoring of stator and rotor windings," pp. 389-437, 2014. https://doi.org/10.1002/9781118886663.ch16

[10] G. Jagadanand, F. L. Dias, "ARM based induction motor fault detection using wavelet and support vector machine", IEEE International Conference on Signal Processing,

Informatics, Communication and Energy Systems (SPICES), pp. 1-4, 2015. https://doi.org/10.1109/SPICES.2015.7091503

[11] M. A. Khan, T. S. Radwan, M. A. Rahman, "Real-time implementation of wavelet packet transform-based diagnosis and protection of three-phase induction motors", *IEEE Trans. Energy Convers*, vol. 22, no. 3, pp. 647-655, 2007. https://doi.org/10.1109/TEC.2006.882417

[12] S. Mallat, "Wavelet Bases," in A Wavelet Tour of Signal Processing, Third., Elsevier Ltd, pp. 263-376, 2009. https://doi.org/10.1016/B978-0-12-374370-1.00011-2

[13] H. Douglas, P. Pillay, P. Barendse, "The detection of interturn stator faults in doubly-fed induction generators", Conference Record - IAS Annual Meeting (IEEE Industry Applications Society), vol. 2, pp. 1097-1102, 2005.

[14] A. Sapena-Baño, "Condition monitoring of electrical machines using low computing power devices", Int. Conf. Electr. Mach., pp. 1516-1522, 2014. https://doi.org/10.1109/ICELMACH.2014.6960383

[15] S. Das, P. Purkait, D. Dey, S. Chakravorti, "Monitoring of inter-turn insulation failure in induction motor using advanced signal and data processing tools", *IEEE Trans. Dielectr. Electr. Insul.*, vol. 18, no. 5, pp. 746-751, 2002. https://doi.org/10.1109/TDEI.2011.6032830

[16] P. S. Barendse, B. Herndler, M. A. Khan, P. Pillay, "The application of wavelets for the detection of inter-turn faults in induction machines", IEEE Int. Electr. Mach. Drives Conf. IEMDC '09, pp. 1401-1407, 2009. https://doi.org/10.1109/IEMDC.2009.5075386

[17] N. R. Devi, S. A. Gafoor, P. V. R. Rao, "Wavelet ANN based stator internal faults protection scheme for 3-phase induction motor", Proc. 2010 5th IEEE Conf. Ind. Electron. Appl. ICIEA 2010, pp. 1457-1461, 2010.

[18] N. Rama Devi, D. V. Siva Sarma, P. V. Ramana Rao, "Detection of stator incipient faults and identification of faulty phase in three-phase induction motor - simulation and experimental verification", *IET Electr. Power Appl.*, vol. 9, no. 8, pp. 540-548, 2015. https://doi.org/10.1049/iet-epa.2015.0024

[19] N. Laouti, S. Othman, M. Alamir, N. Sheibat, "Combination of Model-based Observer and Support Vector Machines for Fault Detection of Wind Turbines", *Int. J. Autom. Comp.*, vol. 11, no. 3, pp. 274-287, 2015. https://doi.org/10.1007/s11633-014-0790-9

[20] D. A. Asfani, M. H. Purnomo, D. R. Sawitri, "Naïve Bayes classifier for Temporary short circuit fault detection in Stator Winding", 9th IEEE International Symposium on Diagnostics for Electric Machines, Power Electronics and Drives (SDEMPED), pp. 288-294, 2013. https://doi.org/10.1109/DEMPED.2013.6645730

[21] S. Choi, B. Akin, M. M. Rahimian, H. A. Toliyat, "Performance-Oriented Electric Motors Diagnostics in Modern Energy Conversion Systems", *IEEE Transactions on Industrial*

Electronics, vol. 59, no. 2. pp. 1266-1277, 2012. https://doi.org/10.1109/TIE.2011.2158037

[22] G. A. Capolino, J. A. Antonino-Daviu, M. Riera-Guasp, "Modern diagnostics techniques for electrical machines, power electronics, and drives", *IEEE Trans. Ind. Electron.*, vol. 62, no. 3, p. 8, 2015. https://doi.org/10.1109/TIE.2015.2391186

[23] H. Henao, "Trends in Fault Diagnosis for Electrical Machines: A Review of Diagnostic Techniques", *IEEE Ind. Electron. Mag.*, vol. 8, no. 2, pp. 31-42, 2014. https://doi.org/10.1109/MIE.2013.2287651

[24] A. Schmitt, H. Silva, R. Scalassara, P. Goedtel, "Bearing Fault Detection Using Relative Entropy of Wavelet Components and Artificial Neural Networks", pp. 538-543, 2013. https://doi.org/10.1109/DEMPED.2013.6645767

[25] L. Hou, N. W. Bergmann, "Induction motor fault diagnosis using industrial wireless sensor networks and Dempster-Shafer classifier fusion", IECON 2011 - 37th Annual Conference of the IEEE Industrial Electronics Society, pp. 2992-2997, 2011. https://doi.org/10.1109/IECON.2011.6119786

[26] G. Feng, A. Mustafa, J. X. Gu, D. Zhen, F. Gu, A. D. Ball, "The real-time implementation of envelope analysis for bearing fault diagnosis based on wireless sensor network", 19th International Conference on Automation and Computing (ICAC), pp. 1-6, 2013.

[27] E. T. Esfahani, S. Wang, V. Sundararajan, "Multisensor wireless system for eccentricity and bearing fault detection in induction motors", *IEEE/ASME Trans. Mechatronics*, vol. 19, no. 3, pp. 818-826, 2014. https://doi.org/10.1109/TMECH.2013.2260865

[28] Maxim Integrated, "MAX291/MAX292/MAX295/MAX296 8th-Order, Lowpass, Switched-Capacitor Filters", no. Rev 5., pp. 1-10.

[29] L. Buitinck, "API design for machine learning software: experiences from the scikit-learn project", ECML PKDD Workshop: Languages for Data Mining and Machine Learning, pp. 108-122, 2013.

[30] F. Pedregosa, "Scikit-learn: Machine Learning in Python", *J. Mach. Learn. Res*., vol. 12, pp. 2825-2830, 2011.

[31] G. M. Joksimovic, J. Penman, "The detection of inter-turn short circuits in the stator windings of operating motors", *IEEE Trans. Ind. Electron.*, vol. 47, no. 5, pp. 1078-1084, 2000. https://doi.org/10.1109/41.873216

[32] M. A. Delgado Narváez, "Monitoreo y Diagnóstico de Electric Machine Drive Systems (EMDS)", Universidad Nacional de Colombia, 2017.